# Sulphurous negative ions in a fuel-rich, $CH_4$–$O_2$ flame with OCS additive

JOHN M. GOODINGS, KAMAL ELGUINDI, AND DIETHARD K. BOHME
*Department of Chemistry, York University, 4700 Keele Street, Downsview, Ont., Canada M3J 1P3*

Received December 15, 1982

JOHN M. GOODINGS, KAMAL ELGUINDI, and DIETHARD K. BOHME. Can. J. Chem. **61**, 1703 (1983).

Sulphurous negative ions $S^-$, $SH^-$, $SO^-$, $SO_2^-/S_2^-$, $SO_3^-$, $HSO_3^-$, $SO_4^-$, and $HSO_4^-$ were observed when 0.2% of carbonyl sulphide (OCS) was added to a conical, laminar, premixed, fuel-rich (equivalence ratio $\phi = 2.15$) $CH_4$–$O_2$ flame burning at atmospheric pressure. Profiles were obtained of ion concentration vs. distance along the flame axis by sampling the flame through a pinhole into a quadrupole mass spectrometer. Some of the ion signals observed in the flame reaction zone are very large, particularly that for $HSO_4^-$. None of the sulphurous ions detected contain carbon. Of those listed above, only $S^-$, $SH^-$, $SO^-$, and $SO_2^-$ persist downstream through the burnt gas. The sulphurous ions are formed by chemical ionization processes of neutral sulphurous intermediates reacting with the naturally-occurring ions present in any hydrocarbon flame. The ion chemistry is discussed, as is the underlying neutral chemistry of sulphur relevant to the flame environment. The ion profiles show the rapidity with which OCS is oxidized through SH and SO to $SO_2$ even within the reaction zone of this fuel-rich flame. No evidence was obtained for the presence of sulphuric or sulphurous acids, and the presence of $S_2$ was not confirmed.

---

JOHN M. GOODINGS, KAMAL ELGUINDI et DIETHARD K. BOHME. Can. J. Chem. **61**, 1703 (1983).

On a observé des ions sulfureux négatifs: $S^-$, $SH^-$, $SO^-$, $SO_2^-/S_2^-$, $SO_3^-$, $HSO_3^-$, $SO_4^-$ et $HSO_4^-$ lorsqu'on ajoute 0,2% de sulfure de carbonyle (OCS) à la flamme de $CH_4$–$O_2$, conique, laminaire, prémélangée et enrichie (rapport d'équivalence $\phi = 2{,}15$) brûlant à la pression atmosphérique. On a obtenu les profils de la concentration en ions en fonction de la distance le long de l'axe de la flamme en injectant des échantillons de flamme à travers un trou d'épingle dans un spectromètre de masse quadrupolaire. Quelques uns des signaux observés dans la zone de réaction de flamme sont très intenses, particulièrement ceux du $HSO_4^-$. Les ions sulfureux détectés ne contiennent pas de carbone. Parmi ceux mentionnés, seuls $S^-$, $SH^-$, $SO^-$ et $SO_2^-$ existent encore dans le courant gazeux qui brûle. Les ions sulfureux se forment par ionisation chimique des intermédiaires sulfureux neutres qui réagissent avec les ions que l'on trouve habituellement dans n'importe quelle flamme d'hydrocarbure. On discute de la chimie de l'ion en tant que chimie neutre sous-jacente du soufre se rapportant à l'environnement de la flamme. Les profils de l'ion révèlent la rapidité avec laquelle le OCS est oxydé par l'intermédiaire du SH et du SO en $SO_2$ même à l'intérieur de la zone de réaction de cette flamme riche en combustible. On n'a pas de preuve de la présence d'acides sulfuriques ou sulfureux, et on n'a pas pu confirmer la présence de $S_2$.

[Traduit par le journal]

## Introduction

The release of sulphur compounds into the troposphere through the use of sulphur-bearing fossil fuels for industrial and domestic heating, power generation, and transportation constitutes the major man-made sources of air contaminants. The effects on human health and vegetation have long been recognized. Besides being phytotoxic with the obvious damage to plants through acid rain, high levels of sulphur compounds have been linked to a variety of environmental and health problems (1). For example, $SO_2$ is a severe irritant to the eyes, mucous membranes, and skin, the irritant effects being caused by the rapidity with which $SO_2$ forms sulphurous acid on contact with moist surfaces. Present measures to combat $SO_x$ emissions from combustion operations through the selection of low-sulphur fuels or by sulphur removal from the exhaust are costly. The inevitable need to use high-sulphur coal in the future points to the desirability of controlling sulphur emissions at the source.

This work attempts to trace the early chemistry of formation of sulphur compounds in a hydrocarbon flame. Sulphur ions resulting from the reaction of naturally-occurring flame ions with sulphurous neutral species are detected by sampling the flame at atmospheric pressure into a mass spectrometer. These ions, produced from fast ion–molecule reactions, can be used as an in-situ probe of the underlying neutral chemistry of combustion. The objective of this phase of the study is to explore the formation and disappearance of negative sulphurous ions in, and downstream of, the reaction zone of a fuel-rich, $CH_4$–$O_2$ flame doped with 0.2% of carbonyl sulphide (OCS). Pairs of ion concentration profiles are measured along the axis of conical flames with and without OCS additive to reveal the presence of sulphurous ions. Both the neutral chemistry and the ion chemistry of sulphur relevant to the flame are discussed.

## Experimental

All of the ion concentration measurements were performed on the same $CH_4$–$O_2$ flame of fuel-rich composition (equivalence ratio $\phi = 2.15$) whose ion chemistry we have studied extensively in the past (2, 3). It was of the laminar premixed type with a conical luminous reaction zone (height ≈ 5 mm, base diameter ≈ 3 mm, thickness ≈ 0.3 mm) to facilitate ionic sampling along the flame axis into a mass spectrometer. The flame has an adiabatic flame temperature of 2460 K and a burnt gas velocity of approximately 1 m s$^{-1}$. It was stabilized at atmospheric pressure on a simple, tubular, quartz burner (2.3 mm id) surrounded by a flowing argon shield to minimize the entrainment of atmospheric air. For this work, provision was made to add 0.22 mol% of OCS to the premixed gas; it could be added or removed without altering the flame. All gases were used straight from the cylinders without further purification ($CH_4 > 99.0\%$, $O_2 > 99.6\%$, Ar $> 99.9\%$, OCS $> 97.5\%$). The burner was mounted on a motor-driven carriage with accurate axial alignment and calibrated drive providing spatial resolution of ±0.02 mm along the flame axis (designated $z$) for ion profile measurements.

The flame – ion mass spectrometer has been described previously in detail (2). The flame burned against a 60°, conical, chromium, sampling nozzle of orifice diameter ca. 0.1 mm mounted in a water-cooled flange of the type described by Hayhurst and Telford (4). The sampled ions pass through two stages of differential pumping into a quadrupole mass filter. The mass-analyzed ions are detected with a parallel-plate Faraday cage connected to a vibrating reed electrometer having a grid-leak resistance of $10^{11}$ ohms. The ion signal magnitudes in the figures are quoted in volts based on the detected ion current passing through $10^{11}$ ohms. We have adopted a normalization technique different from that used previously. The profiles shown in the figures include a correction for mass discrimination in the filter against ions of high $m/e$ measured at high resolving power (unit resolution); the mass discrimination increases with increasing resolving power. The groups of negative sulphurous ions are sufficiently well spaced such that each group could be measured at very low resolving power as a broad single "peak". The individual $m/e$'s within a group measured at high resolving power are normalized to the signal magnitude of the "peak" at low resolving power. The $H_xSO_4^-$ group yields the largest negative ion signal we have ever observed. The dynamic range of sensitivity of the apparatus is five orders of magnitude. A method has been described (2, 5) for locating a reproducible origin ($z = 0$) in the *flame* (not referred to the burner) corresponding to the downstream edge of the luminous reaction zone on the flame axis. In this way, a family of ion profiles at different mass numbers $m/e$ can be accurately overlaid on the distance scale $z$.

It should be pointed out that some ion signals are subject to distortion during sampling by the mass spectrometer. The flame gas is cooled in passing through the thermal boundary layer surrounding the sampling orifice, and again during the expansion to supersonic velocity which proceeds for a few orifice diameters just inside the sampling nozzle. This can affect the signal ratio of two ions participating in a fast ion–molecule reaction having a reaction time (relaxation time) comparable to, or less than, the sampling time (of order 1 μs). In these circumstances, the ratio will change to some extent during sampling in favour of the product ion in the exothermic direction of the reaction. An extreme case is the production of hydrate ions, since a large water concentration in the flame produces a high rate of hydration. In the present study where some of the sulphurous ions of relatively high molecular weight may result from clustering reactions with sulphur dioxide, their signals may be enhanced by cooling during sampling. However, such enhancements are not expected to affect the interpretation of the sulphurous flame chemistry. These sampling effects for flames have been discussed in a series of papers by Hayhurst *et al.* of which refs. 6–8 are particularly relevant.

## Neutral sulphur chemistry in hydrocarbon flames

A complete review of the reactions of neutral sulphurous species will not be attempted here. However, relevant reactions studied by a number of workers are listed in Table 1; where the temperature dependence is known, the rate constants have been calculated at 2000 K. The reactions are drawn from Westley's table of recommended rate constants for chemical reactions occurring in combustion (9). The sulphur chemistry is summarized in the reaction flow diagram given in Fig. 1.

Initially, the OCS additive is attacked by O and H atoms to form SO and SH, respectively (reactions [1] and [2]), whose rates may be nearly equal in our flame. In any case, SH is rapidly attacked by O in reaction [4*a*] to yield the same SO product. In turn, SO can react with $O_2$ or O (reactions [5*a*] and [6]) to give the major product $SO_2$. The back reaction [5*b*] can regenerate SO from $SO_2$, but should be very slow early in the reaction zone. The reaction of H with $SO_2$ does not regenerate SO, but adds rather slowly [7] to form $HSO_2$. This completes what might be regarded as the main-line sulphur chemistry; namely,

$$\text{OCS} \rightarrow (\text{SH}) \rightarrow \text{SO} \rightarrow \text{SO}_2$$

Sulphur is further involved in minor side-line chemistry. Sulphur atoms can be produced by H and O radical attack on both SO and SH (reactions [8*c*], [9*a*], [10*a*], and [4*b*]). However, SO is regenerated by reaction of S atoms with $O_2$ by [9*b*] or with OH by [8*a*]. The regeneration rate of SH by reaction [10*b*] involving S with $H_2$ may be comparable downstream despite its small rate constant due to the high concentration of $H_2$ (0.4 mole fraction) in the fuel-rich burnt gas (2).

As a second side-line, diatomic sulphur $S_2$ can be formed by reaction [11*a*] of S with SH, but is destroyed by the reverse reaction [11*b*] with H atoms. A further sink for $S_2$ is its reaction [12*b*] with O atoms to form SO; the reverse reaction [12*a*] as a source of $S_2$ can be disregarded. Reaction [3] of OCS with S is a significant source of $S_2$ only if the concentration of S becomes appreciable before OCS is exhausted. Thus, $S_2$ feeds back rapidly into the main-line sulphur chemistry, and its steady-state concentration in the fuel-rich flame is expected to be low.

A third side-line concerns $H_2S$. The only reaction listed by Westley (9) for its production is [13] involving the reaction of the SH radical with itself. However, several sink reactions are known for the destruction of $H_2S$ by H, OH, and $CH_3$ radicals (reactions [14], [15], and [16], respectively). As an aside, we do have evidence for the presence of $H_2S$ in the flame from the positive ion chemistry where we detect $H_3S^+$, presumably arising from proton transfer to $H_2S$. Under the fuel-rich flame conditions, it is possible that the reverse of reaction [14] constitutes the major source of $H_2S$ since the concentration of $H_2$ is high in the burnt gas.

An obvious question is the degree to which the reactions are balanced in different parts of the flame linking the pairs of species $SH/H_2S$, SH/S, $S_2/S$, SO/S, and $SO/SO_2$. An indication is given by some of the ion profiles below which show a similar tailing out downstream in the burnt gas. It will be noted that Table 1 and Fig. 1 do not mention any sulphurous species containing carbon. Their inclusion is not thought to be warranted because, in general, the rates of reactions listed in Westley (9) of C, CH, $CH_2$, etc. with sulphurous species are low due to the small steady-state concentrations of the hydrocarbon neutrals. Also, addition reactions similar to [7] are known from the chemistry of the stratosphere near 220 K for the formation of $HSO_3$ from OH + $SO_2$ + M, and $SO_3$ from O + $SO_2$ + M (13, 14); the $SO_3$ so formed combines with water to form sulphuric acid. However, we do not have any evidence for these processes occurring at flame temperatures.

## Results

Figure 2 shows total positive and total negative ion profiles with, and without, the injection of 0.2% of OCS into the premixed flame gas. In these and subsequent ion profile data, the conical flame is sampled into the mass spectrometer along its axis (distance $z$ in mm); the flame reaction zone near the tip of the cone occupies the region from approximately $z = -0.3$ to 0 mm. The total positive ion profile shows little change in magnitude or peak shape with OCS injection. However, the total negative ion profile shows a dramatic increase in magnitude of the upstream peak (4. 5 ×) with the addition of 0.2% of OCS and a much greater persistance of the downstream peak into the burnt gas region of the flame.

Figures 3–7 inclusive present profiles for sulphurous negative ion species at individual $m/e$. Each figure gives data for a group of similar ions; the groups are ordered according to increasing mass. Figure 3 shows profiles for the $H_xS^-$ group ($x$ = 0, 1). In the absence of OCS, the profile at 32 amu is due to $O_2^-$, and shows a single peak upstream. With OCS injection, the profile becomes double-peaked. The upstream peak falls to a magnitude of one-third and shifts slightly in the downstream direction; evidently $O_2^-$ acts as a source or reagent ion for the production of sulphurous negative ions by ion–molecule reactions. In addition, a new peak due to $S^-$ appears downstream and tails out into the burnt gas. It is apparent from this and other profiles which show similar tailing behaviour that some of the sulphurous negative ions involve species of relatively high

TABLE 1. Neutral reactions involving sulphurous species relevant to the fuel-rich hydrocarbon flame doped with OCS

| No. | Reactions | Rate constant[a] | $T$ (K)[b] | Reference |
|---|---|---|---|---|
| [1] | $O + OCS \rightarrow SO + CO$ | [d]$4.1 \times 10^{-12}$ | 1 200 | 10 |
| [2] | $H + OCS \rightarrow SH + CO$ | [e]$2.2 \times 10^{-14}$ | 298 | 10 |
| [3] | $S + OCS \rightarrow S_2 + CO$ | [e]$1.0 \times 10^{-12}$ | 2 000 | 10 |
| [4*a*] | $SH + O \rightarrow SO + H$ | $4.7 \times 10^{-11}$ | 2 000 | 11 |
| [4*b*] | $\rightarrow S + OH$ | $1.4 \times 10^{-13}$ | 2 000 | 11 |
| [5*a*] | $SO + O_2 \rightarrow SO_2 + O$ | [e]$1.5 \times 10^{-13}$ | 2 000 | 10 |
| [5*b*] | $SO_2 + O \rightarrow SO + O_2$ | [e]$3.3 \times 10^{-14}$ | 2 000 | 10 |
| [6] | $SO + O + M \rightarrow SO_2 + M$ | [e]$1.8 \times 10^{-31}$ | 298 | 10 |
| [7] | $H + SO_2 + M \rightarrow HSO_2 + M$ | [d]$1.4 \times 10^{-32}$ | 2 000 | 10 |
| [8*a*] | $S + OH \rightarrow SO + H$ | $4.7 \times 10^{-11}$ | 2 000 | 11 |
| [8*b*] | $\rightarrow SH + O$ | $1.7 \times 10^{-13}$ | 2 000 | 11 |
| [8*c*] | $SO + H \rightarrow S + OH$ | $1.1 \times 10^{-12}$ | 2 000 | 11 |
| [9*a*] | $SO + O \rightarrow S + O_2$ | $3.7 \times 10^{-12}$ | 2 000 | 11 |
| [9*b*] | $S + O_2 \rightarrow SO + O$ | [e]$2.3 \times 10^{-12}$ | 250–450 | 10 |
| [10*a*] | $SH + H \rightarrow S + H_2$ | [d]$2.5 \times 10^{-11}$ | 298 | 10 |
| [10*b*] | $S + H_2 \rightarrow SH + H$ | [d]$2.0 \times 10^{-13}$ | 2 000 | 10 |
| [11*a*] | $S + SH \rightarrow S_2 + H$ | $4.7 \times 10^{-11}$ | 2 000 | 11 |
| [11*b*] | $S_2 + H \rightarrow S + SH$ | $9.0 \times 10^{-12}$ | 2 000 | 11 |
| [12*a*] | $S + SO \rightarrow S_2 + O$ | $1.5 \times 10^{-13}$ | 2 000 | 11 |
| [12*b*] | $S_2 + O \rightarrow S + SO$ | $4.7 \times 10^{-11}$ | 2 000 | 11 |
| [13] | $SH + SH \rightarrow H_2S + S$ | [d]$1.3 \times 10^{-11}$ | 295 | 10 |
| [14] | $H_2S + H \rightarrow SH + H_2$ | [d]$2.1 \times 10^{-12}$ | 470 | 10 |
| [15] | $H_2S + OH \rightarrow SH + H_2O$ | [e]$8.4 \times 10^{-12}$ | 900 | 10 |
| [16] | $H_2S + CH_3 \rightarrow SH + CH_4$ | $1.1 \times 10^{-14}$ | 600 | 12 |

[a] Rate constants are given in units of $cm^3$ $molecule^{-1}$ $s^{-1}$, or $cm^6$ $molecule^{-2}$ $s^{-1}$ where appropriate.
[b] Each rate constant has been calculated at a temperature as close to 2 000 K as the available data permit.
[c] Approximate uncertainty ≃ ±30%.
[d] Approximate uncertainty ≃ ±50%.
[e] Approximate uncertainty ≃ ±70%.

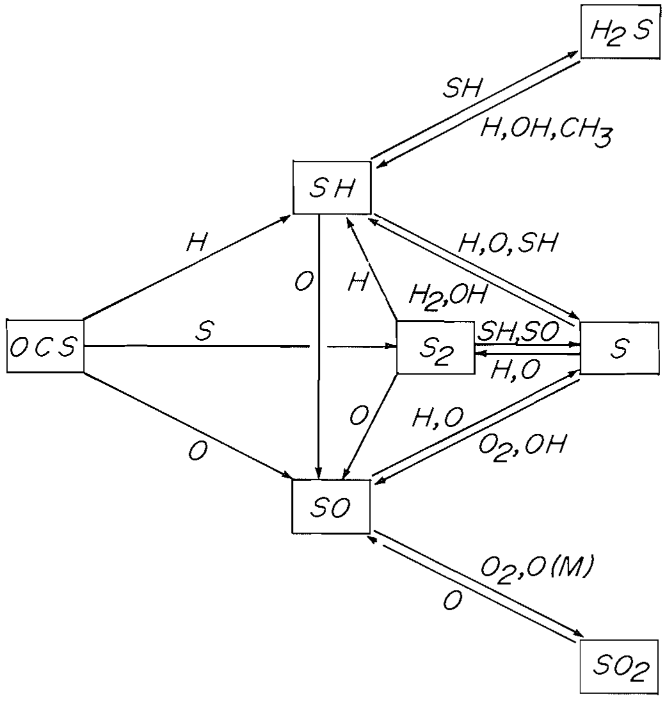

FIG. 1. Reaction scheme for sulphur chemistry in a fuel-rich, hydrocarbon flame.

electron affinity (EA) which can better withstand collisional electron detachment at the high temperature of the burnt gas.

In the absence of OCS, a small single peak is observed at 33 amu in the reaction zone due to $HO_2^-$. With OCS injection, the much larger double-peaked profile shown in Fig. 3 arises due to $SH^-$ with a small contribution from $^{33}S^-$. Recall that sulphur has four stable isotopes: namely, $^{32}S$ (natural abundance = 95.0%), $^{33}S$ (0.76%), $^{34}S$ (4.22%), and $^{36}S$ (0.014%). Other isotopic species of sufficient natural abundance to make significant contributions to some of these profiles include deuterium D (0.015%), $^{17}O$ (0.037%), and $^{18}O$ (0.0204%). For example, the double-peaked profile at 34 amu can be derived from $^{32}SD^-$, $^{34}S^-$, and $^{33}SH^-$; these sulphurous species will account for all of the downstream portion, whereas the upstream peak is further complicated by a small and unknown contribution from the $O^-.H_2O$ hydrate. Similar considerations will apply to the profile at 35 amu, but in this case the profile magnitude indicates contributions from $OH^-.H_2O$ and also $^{35}Cl^-$ present as an impurity. The mass assignments including isotopic contributions for all of the negative sulphurous ion profiles measured are summarized by groups in Table 2.

Consider now the small, double-peaked profiles at 48 amu shown in Fig. 4. In the absence of OCS, the upstream and downstream peaks are attributed to $O_3^-$ and $C_4^-$, respectively. With OCS injection, the decrease and shift of the upstream peak presumably indicates the involvement of $O_3^-$ as a source of sulphurous negative ions, as noted above for $O_2^-$. The increase in the downstream peak may be indicative of $SO^-$. However, the clear evidence for $SO^-$ is the tail of the profile which persists far downstream into the burnt gas. Corroborative evidence from $^{34}SO^-$ at 50 amu is obscured by the presence of $O_2^-.H_2O$.

With reference to Fig. 5, in the absence of OCS, the signal detected at 64 amu is negligible and that at 66 amu is very small. With OCS injection, the fairly large profile at 64 amu

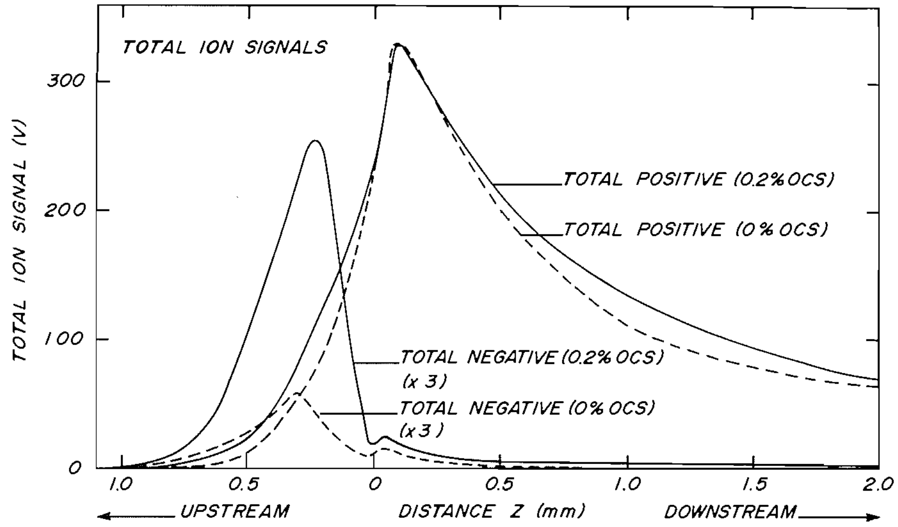

FIG. 2. Total positive and negative ion profiles with, and without, 0.2% OCS additive.

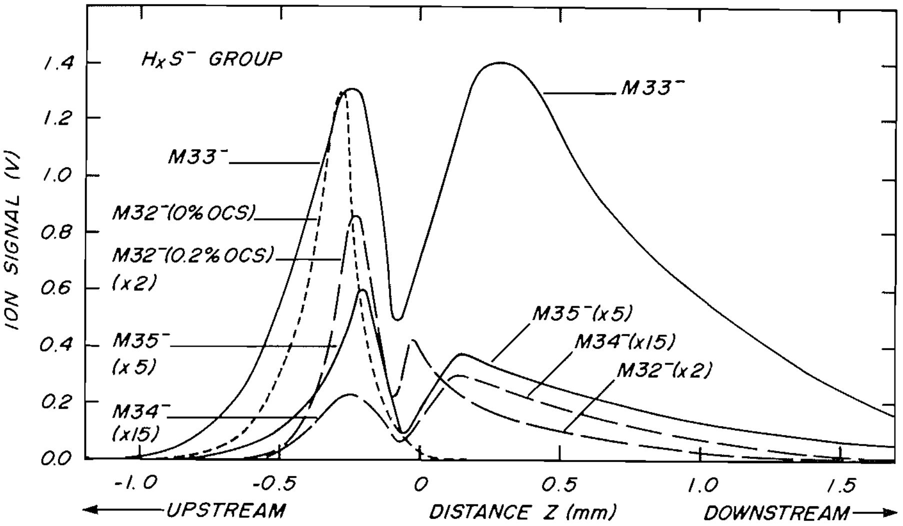

FIG. 3. Negative sulphurous ion profiles: isotopic species of S and SH. All profiles are taken with the addition of 0.2% of OCS except for one profile at −32 amu as indicated.

could be attributed to $SO_2^-$ or $S_2^-$. However, the relative size and similar shape of the profile at 66 amu identifies both peaks as being almost entirely due to $SO_2^-$ and not $S_2^-$; this serves as an excellent example of the utility of isotopes for species identification.

The $H_xSO_3^-$ group ($x$ = 0, 1) of ions is shown in Fig. 6. When OCS is not present, the signals at 80–83 amu are all negligibly small. When 0.2% of OCS is added, large profiles are observed. The single-peaked pair at 80 and 82 amu are attributed to $^{32}SO_3^-$ and $^{34}SO_3^-$, respectively; the latter contains minor contributions from other isotopic species as well. The double-peaked pair of profiles at 81 and 83 amu are identified mainly as $H^{32}SO_3^-$ and $H^{34}SO_3^-$, respectively, although other isotopic species will contribute. As a clue to the ion chemistry dicussed in the next section, it is noteworthy that the profile observed for $O^-$ at 16 amu (not shown here) is single-peaked, while that for $OH^-$ at 17 amu (also not shown) is double-peaked (15). Thus, it is credible that the ions observed in this group are the cluster ions $O^-.SO_2$ and $OH^-.SO_2$.

Similarly for the $H_xSO_4^-$ group ($x$ = 0, 1) of ions shown in Fig. 7, the signals at 96–99 amu with OCS absent were negligibly small. With OCS injection, sulphurous negative ion profiles were observed, all single-peaked and one of them very large. They derive, in order of increasing mass 96–99 amu, from $^{32}SO_4^-$, $H^{32}SO_4^-$, $^{34}SO_4^-$, and $H^{34}SO_4^-$ with a number of other isotopic contributions indicated in Table 2. In fact, the peak for $HSO_4^-$ at 97 amu is the largest negative ion signal we have ever observed. In the absence of OCS, the profile for $O_2^-$ at 32 amu (Fig. 3) and the very small one for $HO_2^-$ at 33 amu (not shown) are both single-peaked (15). In keeping with the cluster ion interpretation mentioned in the previous paragraph, the $H_xSO_4^-$ ions might conceivably arise as $O_2^-.SO_2$ and $HO_2^-.SO_2$ clusters.

In summary, the parent negative ions for which profiles were obtained include $S^-$, $SH^-$, $SO^-$, $SO_2^-(S_2^-)$, $SO_3^-$, $HSO_3^-$, $SO_4^-$, and $HSO_4^-$. Somewhat surprisingly, we were unable to obtain any evidence for sulphurous negative ions containing carbon in the fuel-rich flame.

## Discussion of the sulphurous negative ion chemistry

It remains to discuss the probable ion–molecule reactions which are relevant to the sulphurous negative ions observed.

TABLE 2. Relative isotopic contributions of sulphurous negative ion groups above mass number *M* amu

| Parent ion | *M* | | *M* + 1 | | *M* + 2 | | *M* + 3 | |
|---|---|---|---|---|---|---|---|---|
| *$H_xS^-$ group:* M = *32* | | | | | | | | |
| $S^-$ | $^{32}S$ | [a](1) | $^{33}S$ | [b](0.0080) | $^{34}S^-$ | (0.0444) | | |
| $SH^-$ | | | $^{32}SH$ | (1) | $^{33}SH^-$ | (0.0080) | $^{34}SH$ | (0.0444) |
| Other ions | $O_2^-$ | | $HO_2$ | | $O^-.H_2O$ | | $OH^-.H_2O$; $^{35}Cl$ | |
| *$SO^-$ group:* M = *48* | | | | | | | | |
| $SO^-$ | $^{32}S^{16}O^-$ | (1) | | | $^{34}S^{16}O^-$<br>$^{32}S^{18}O^-$ | (0.0444)<br>(0.0020) | | |
| Other ions | $O_3^-$; $C_4^-$ | | | | $O_2^-.H_2O$; $C_4H_2^-$ | | | |
| *$SO_2^-/S_2^-$ group:* M = *64* | | | | | | | | |
| $SO_2^-$ | $^{32}S^{16}O_2^-$ | (1) | | | $^{34}S^{16}O_2^-$<br>$^{32}S^{18}O^{16}O^-$ | (0.0444)<br>(0.0041) | | |
| $S_2^-$ | $^{32}S_2^-$ | (1) | | | $^{34}S^{32}S^-$ | (0.0888) | | |
| *$H_xSO_3^-$ group:* M = *80* | | | | | | | | |
| $SO_3^-$ | $^{32}S^{16}O_3^-$ | (1) | $^{33}S^{16}O_3^-$<br>$^{32}S^{17}O^{16}O_2^-$ | (0.0080)<br>(0.0011) | $^{34}S^{16}O_3^-$<br>$^{32}S^{18}O^{16}O_2^-$ | (0.0444)<br>(0.0061) | | |
| $HSO_3^-$ | | | $H^{32}S^{16}O_3^-$ | (1) | $H^{33}S^{16}O_3^-$<br>$H^{32}S^{17}O^{16}O_2^-$ | (0.0080)<br>(0.0011) | $H^{34}S^{16}O_3$<br>$H^{32}S^{18}O^{16}O_2$ | (0.0444)<br>(0.0061) |
| Other ions | | | | | | | $SO_2^-.H_2O$ | |
| *$H_xSO_4^-$ group:* M = *96* | | | | | | | | |
| $SO_4^-$ | $^{32}S^{16}O_4^-$ | (1) | $^{33}S^{16}O_4^-$<br>$^{32}S^{17}O^{16}O_3^-$ | (0.0080)<br>(0.0015) | $^{34}S^{16}O_4^-$<br>$^{32}S^{18}O^{16}O_3^-$ | (0.0444)<br>(0.0082) | | |
| $HSO_4^-$ | | | $H^{32}S^{16}O_4^-$ | (1) | $H^{33}S^{16}O_4^-$<br>$H^{32}S^{17}O^{16}O_3^-$ | (0.0080)<br>(0.0015) | $H^{34}S^{16}O_4$<br>$H^{32}S^{18}O^{16}O_3$ | (0.0444)<br>(0.0082) |
| Other ions | $S^-.SO_2$; $S_3^-$ | | $SH^-.SO_2$; $SH^-.S_2$ | | $SO_3^-.H_2O$ | | $HSO_3^-.H_2O$ | |

[a] The parent ion composed of the most probable isotopes is designated unity (1).

[b] Relative contributions of less probable isotopic species are included which contribute >0.1% of unity (1).

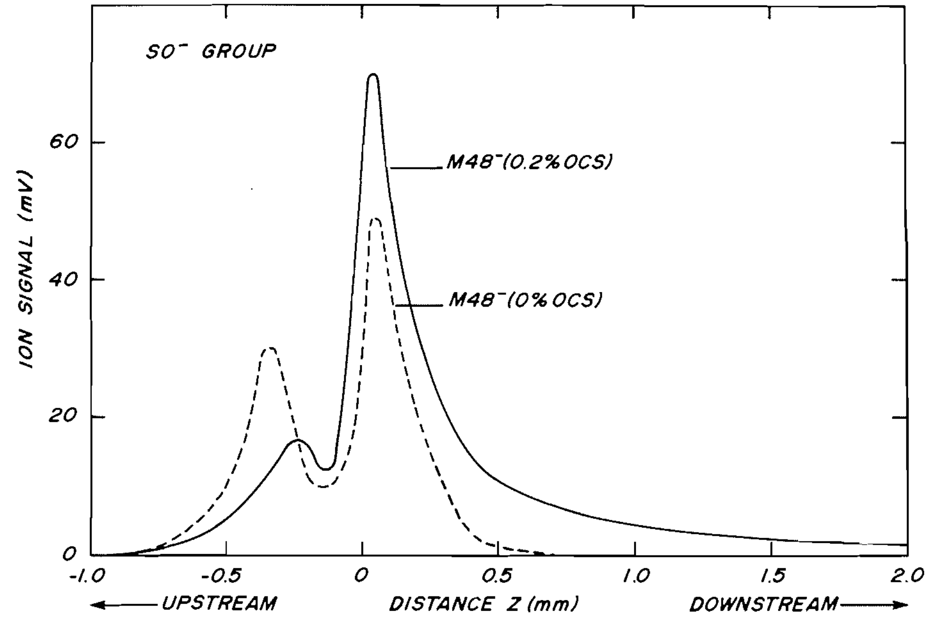

FIG. 4. Negative sulphurous ion profiles: $SO^-$.

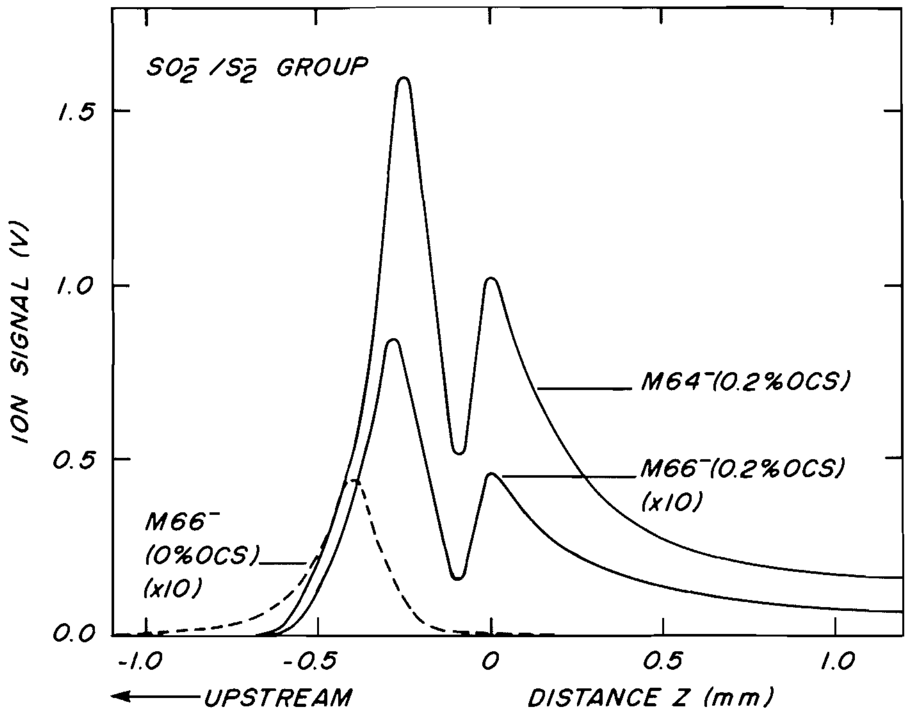

FIG. 5. Negative sulphurous ion profiles: isotopic species of $SO_2^-$ ($S_2^-$). Also shown is the signal at −66 amu in the absence of OCS additive.

Those which have been studied previously by other workers, usually at room temperature, are listed in Table 3. Many are drawn from the compilation by Albritton (16). The discussion of the ion chemistry reveals the sulphurous neutral species expected to be present in the flame as intermediates and products.

There is general agreement that the main primary source of ions in a hydrocarbon flame is the chemi-ionization reaction (27, 28)

[17] $CH + O \rightarrow HCO^+ + e^-$

The negative ion chemistry commences upstream with three-body attachment of the electrons released in reaction [17] to $O_2$ molecules (3)

[18] $e^- + O_2 + M \rightarrow O_2^- + M$

In this study, one might expect sulphurous negative ions to arise initially by dissociative electron attachment to OCS. There are five plausible reaction channels to form $O^-$, $C^-$, $S^-$, $SO^-$, and $CS^-$; for example

[19] $e^- + OCS \rightarrow S^- + CO$

Although some of them have been observed at relatively high energies using electron beams (29, 30), all will be endothermic

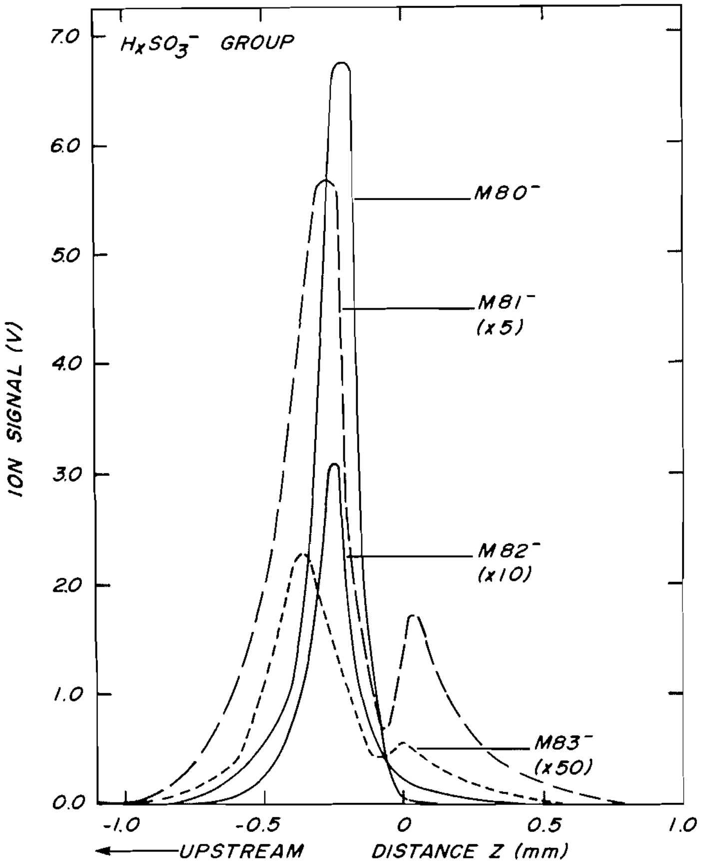

FIG. 6. Negative sulphurous ion profiles: isotopic species of $SO_3^-$ and $HSO_3^-$. All profiles are taken with the addition of 0.2% of OCS.

at normal flame temperatures. Of the five, reaction [19] is the most favourable with an endothermicity of approximately 25 kcal $mol^{-1}$.

However, several of the sulphurous neutrals invoked in Fig. 1 have electron affinities (EA) greater than that of $O_2$, and can give rise to some of the observed sulphurous ions by charge transfer reactions

[20] $O_2^- + SH \rightarrow SH^- + O_2$ EA(SH) = 2.319 eV (31)

[21] $+ SO \rightarrow SO^- + O_2$ EA(SO) = 1.09 eV (32)

[22] $+ SO_2 \rightarrow SO_2^- + O_2$ $EA(SO_2)$ = 1.097 eV (33)

[23] $+ S \rightarrow S^- + O_2$ EA(S) = 2.077 eV (34)

Reaction [22] has a high rate constant measured at 300 K given in Table 3. It is perhaps significant that $SH^-$ (Fig. 3) and $SO^-$ (Fig. 4) originate farther upstream than do $SO_2^-$ (Fig. 5) and $S^-$ (Fig. 6) in keeping with the sequence of neutral reactions presented in Fig. 1. Also, $SH^-$ could logically be formed by proton transfer from $H_2S$ to a strong base such as $OH^-$

[24] $OH^- + H_2S \rightarrow SH^- + H_2O$

It is not possible to differentiate between $SH^-$ formed by proton transfer from $H_2S$ or by charge transfer to SH. In addition, $SO_2^-$ and $SO^-$ could be formed by atom transfer reactions

[25] $O_2^- + OCS \rightarrow SO_2^- + CO$

[26] $\rightarrow SO^- + CO_2$

Both are exothermic, although reaction [26] involves a good deal of chemical rearrangement.

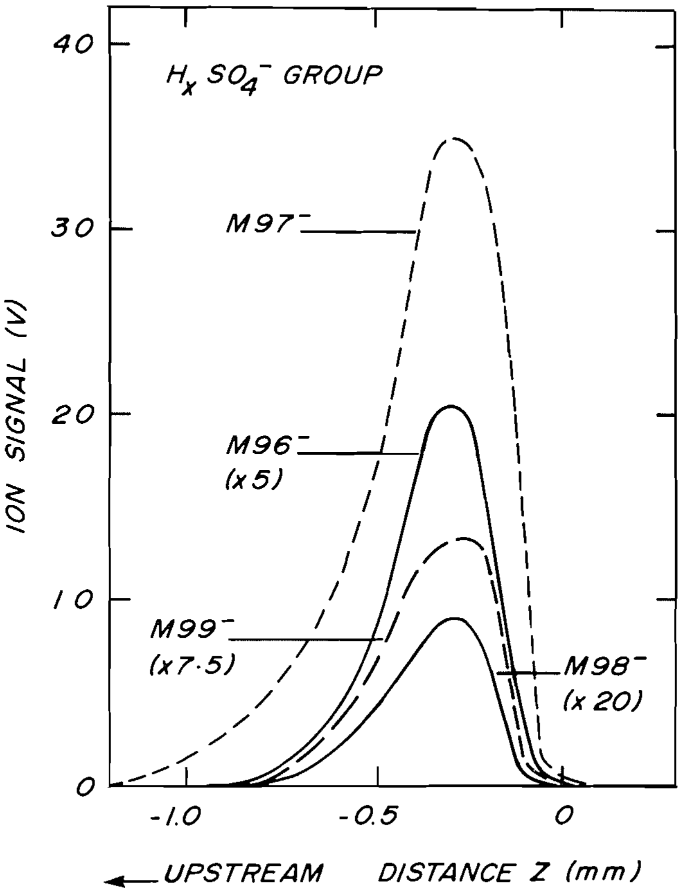

FIG. 7. Negative sulphurous ion profiles: isotopic species of $SO_4^-$ and $HSO_4^-$. All profiles are taken with the addition of 0.2% of OCS.

As was mentioned in presenting the Results for the $H_xSO_3^-$ and $H_xSO_4^-$ groups, some of the remaining sulphurous ions can be formed in clustering reactions with $SO_2$

[27] $OH^- + SO_2 + M \rightarrow HSO_3^- + M$

[28] $HO_2^- + SO_2 + M \rightarrow HSO_4^- + M$

$EA(HSO_4) > 4.5$ eV (21)

Reaction [27] has the very high rate constant measured at 296 K given in Table 3. Viggiano *et al.*'s determination (21) of a lower limit for $EA(HSO_4)$ based on Benson's somewhat uncertain value (35) for the bond dissociation energy of sulphuric acid $D(H{-}HSO_4) = 4.5$ eV means that dissociative electron attachment to $H_2SO_4$

[29] $e^- + H_2SO_4 \rightarrow HSO_4^- + H$

would be exothermic, certainly near room temperature. The fact that the $HSO_4^-$ profile (Fig. 7) does not persist downstream is strong evidence that sulphuric acid is not a major product in the burnt gas of the flame. The very large signals obtained for $HSO_4^-$ in the reaction zone are not surprising in view of the very high values of $EA(HSO_4)$; once $HSO_4^-$ forms by $SO_2$ clustering according to reaction [28], it will be very stable against loss by charge transfer to SH, SO, $SO_2$, etc. Also, if $HSO_4^-$ is formed in the reaction zone by proton abstraction from $H_2SO_4$ by the strong base $OH^-$

[30] $OH^- + H_2SO_4 \rightarrow HSO_4^- + H_2O$

the $HSO_4^-$ profile ought to be double-peaked like that for $OH^-$

TABLE 3. Ion–molecule reactions involving sulphurous species relevant to the fuel-rich flame doped with OCS

| No. | Reactions | [a]Rate constant | Temperature or energy | Reference |
|---|---|---|---|---|
| [22] | $O_2^- + SO_2 \rightarrow SO_2^- + O_2$ | [b]$1.9 \times 10^{-9}$ | 303 K | 17 |
| | | $3.9 \times 10^{-9}$ | 0.13 eV | 18 |
| [27] | $OH^- + SO_2 + O_2 \rightarrow HSO_3^- + O_2$ | [b]$1.0 \times 10^{-26}$ | 296 K | 19 |
| [31] | $CO_3^- + SO_2 \rightarrow SO_3^- + CO_2$ | [b]$4.0 \times 10^{-10}$ | 0.04–1.9 eV | 20 |
| | | [b]$3.5 \times 10^{-10}$ | 185–605 K | 20 |
| [32] | $HCO_3^- + SO_2 \rightarrow HSO_3^- + CO_2$ | [b]$1.7 \times 10^{-9}$ | 296 K | 19 |
| [33] | $O_3^- + SO_2 \rightarrow SO_3^- + O_2$ | [b]$1.7 \times 10^{-9}$ | 0.04–1.8 eV | 20 |
| | | [b]$1.7 \times 10^{-9}$ | 185–605 K | 20 |
| [34] | $O_2^-.H_2O + SO_2 \rightarrow SO_4^- + H_2O$ | [b]$1.8 \times 10^{-9}$ | 303–304 K | 17 |
| [35] | $O^- + H_2SO_4 \rightarrow HSO_4^- + OH$ | [d]$1.54 \times 10^{-9}$ | 343 K | 21 |
| [36] | $SO_2^- + O_2 + O_2 \rightarrow SO_4^{-*} + O_2$ | [e]Observed | 296 K | 19 |
| [37*a*] | $SO_4^{-*} + H \rightarrow HO_2^- + SO_2$ | [c]$1.6 \times 10^{-10}$ | 296 K | 22 |
| [37*b*] | $\rightarrow SO_2^- + HO_2$ | $SO_2^-$ was the major product ion | | |
| [38] | $S^- + CO \rightarrow e^- + OCS$ | [b]$3.1 \times 10^{-10}$ | 300 K | 23 |
| [39] | $S^- + O_2 \rightarrow e^- + SO_2$ | [b]$3 \times 10^{-11}$ | 300 K | 24 |
| | $S^- + H_2 \rightarrow e^- + H_2S$ | $<1 \times 10^{-15}$ | 300 K | 24 |
| [40] | $SH^- + H \rightarrow e^- + H_2S$ | [d]$1.3 \times 10^{-9}$ | 296 K | 25 |
| [41*a*] | $O^- + SO_2 \rightarrow e^- + SO_3$ | $2.0–0.8 \times 10^{-9}$ | 0.05–0.28 eV | 18 |
| [41*a*] | $O^- + SO_2 \rightarrow e^- + SO_3$ | $2.1 \times 10^{-9}$ | 0.04–2.0 eV | 26 |
| [41*b*] | $\rightarrow SO_2^- + O$ | Major channel at higher energies | | |

[a]Rate constants are given in units of $cm^3$ $molecule^{-1}$ $s^{-1}$, or $cm^6$ $molecule^{-2}$ $s^{-1}$ where appropriate.
[b]The measurement uncertainty is ±30%.
[c]The measurement uncertainty is ±40%.
[d]The measurement uncertainty is +100%, −50%.
[e]$SO_4^{-*}$ designates the less stable isomer of $SO_4^-$.

or $HSO_3^-$. Presumably $HSO_4^-$ is lost near the end of the reaction zone because the flame attains maximum temperature and the H atom concentration rises (2, 36), both of which favour associative detachment of electrons by the reverse (endothermic) direction of reaction [29]. All things considered, the large signal detected for $HSO_4^-$ does not provide evidence for the presence of sulphuric acid in the flame. It probably forms, however, in the cool, wet, gaseous envelope surrounding the flame proper.

Other ion–molecule reactions listed in Table 3 have been measured which can form ions of the $H_xSO_3^-$ and $H_xSO_4^-$ groups. Some of these might be regarded as switching reactions or anion transfer

[31] $CO_3^-(O^-.CO_2) + SO_2 \rightarrow SO_3^-(O^-.SO_2) + CO_2$

[32] $HCO_3^-(OH^-.CO_2) + SO_2 \rightarrow HSO_3^-(OH^-.SO_2) + CO_2$

[33] $O_3^-(O^-.O_2) + SO_2 \rightarrow SO_3^-(O^-.SO_2) + O_2$

[34] $O_2^-.H_2O + SO_2 \rightarrow SO_4^-(O_2^-.SO_2) + H_2O$

Certainly all of the reagent ions in reactions [31]–[34] have been observed in the fuel-rich flame with OCS absent (3, 15). In addition, a fast proton transfer reaction akin to [30] involving $O^-$ as the proton acceptor has been measured (21)

[35] $O^- + H_2SO_4 \rightarrow HSO_4^- + OH$

Also, $SO_4^-$ can be produced by a clustering reaction of $SO_2^-$ with $O_2$

[36] $SO_2^- + O_2 + O_2 \rightarrow SO_4^{-*} + O_2$

although the less stable isomer of $SO_4^-$ is formed, designated $SO_4^{-*}$ (19). Its reaction with H atoms has been observed to produce two channels (22)

[37*a*] $SO_4^{-*} + H \rightarrow HO_2^- + SO_2$

[37*b*] $\rightarrow SO_2^- + HO_2$ major channel at 296 K

Many other reactions involving the $H_xSO_3^-$ and $H_xSO_4^-$ ions undoubtedly exist, but have not been measured to date.

Several examples involving the loss of sulphurous species by associative electron detachment have been measured

[38] $S^- + CO \rightarrow e^- + OCS$

[39] $S^- + O_2 \rightarrow e^- + SO_2$

[40] $SH^- + H \rightarrow e^- + H_2S$

[41*a*] $O^- + SO_2 \rightarrow e^- + SO_3$

[41*b*] $\rightarrow SO_2^- + O$ major channel at high energy

Reactions [38]–[40] have been measured at room temperature. The behaviour of reaction [41] as a function of energy or temperature may by typical and significant for flames. Although associative detachment may dominate at room temperature, a different ion–molecule reaction channel may become the major one at high temperature; e.g. charge transfer in the case of reaction [41]. In general, most of the sulphurous negative ions observed are logical candidates for associative detachment reactions with prominent flame neutrals such as H, O, OH, $H_2$, CO, etc. It is difficult to imagine that such reactions have large rate constants at flame temperatures in view of the large signals obtained for most of the sulphurous negative ions observed.

With regard to the burnt gas region downstream, the $HSO_3^-$ profile (Fig. 6) persists to some extent in keeping with the interpretation of its formation as a cluster ion of $OH^-$ with $SO_2$ by reaction [27]. The similarity to the $OH^-$ profile was mentioned near the end of the section on Results. However, four of the ion profiles ($S^-$ and $SH^-$ in Fig. 3, $SO^-$ in Fig. 4 and $SO_2^-$ in Fig. 5) persist far downstream through the burnt gas where no negative ions are detected in the same flame with OCS absent. From the electron affinities given beside reactions [20]–[23], a mechanism can be envisaged involving formation by three-body electron attachment primarily to $SO_2$, with subsequent charge transfer to SH, S, and SO, balanced by loss processes involving associative electron detachment with H, O, and CO, and collisional detachment. Such a network of reactions is reasonable to account for the persistent steady-state profiles observed for these four ionic species. It is consistent with the presence throughout the burnt gas of the sulphurous neutral species, SH, SO, $SO_2$, and S.

## Conclusions

A number of conclusions may be drawn from this work pertaining to both the ion chemistry and the neutral chemistry of sulphur in flames.

*Ion chemistry*

(*1*) Most of the sulphurous negative ion chemistry seems to be understandable in terms of the relatively few ion–molecule reactions involving sulphurous species measured to date near room temperature.

(*2*) Negative ion clustering and switching (or anion transfer) reactions with $SO_2$ appear to be prominent.

(*3*) None of the sulphurous negative ions detected contain carbon, even under fuel-rich conditions.

(*4*) For analytical purposes concerned with the mass-spectrometric monitoring of sulphur in flames, very large signals of $HSO_4^-$ were detected around the flame reaction zone. Persisting downstream through the burnt gas, $SH^-$ and $SO_2^-$ are the logical candidates.

*Neutral chemistry*

(*5*) The profiles show that all of the expected sulphur compounds — $SH(H_2S)$, SO, $SO_2(S_2)$, S — are present *early in the flame reaction zone*. The rates of the chemical reactions summarized in Fig. 1 which interconvert these species must be fast in the flame environment, since OCS is rapidly oxidized to $SO_2$ even under fuel-rich conditions.

(*6*) The main-line neutral sulphur chemistry in the flame appears to follow the sequence $OCS \rightarrow (SH) \rightarrow SO \rightarrow SO_2$. The species S, $S_2$, and $H_2S$ are involved in chemical side-lines. No direct evidence was obtained for $S_2$, however.

(*7*) No evidence was obtained for $H_2SO_4$ or $H_2SO_3$ in the flames proper, although they will undoubtedly form in the cooler, wet region adjacent to the combustion envelope.

1. A. G. COOPER. Sulphur oxides and other sulphur compounds, a bibliography with abstracts. U.S. Dept. of Health Education and Welfare, Washington, DC. 1965.
2. J. M. GOODINGS, D. K. BOHME, and C.-W. NG. Combust. Flame, **36**, 27 (1979).
3. J. M. GOODINGS, D. K. BOHME, and C.-W. NG. Combust. Flame, **36**, 45 (1979).
4. A. N. HAYHURST and N. R. TELFORD. Combust. Flame, **28**, 67 (1977).
5. D. K. BOHME, J. M. GOODINGS, and C.-W. NG. Int. J. Mass Spectrom. Ion Phys. **24**, 335 (1977).
6. A. N. HAYHURST and D. B. KITTELSON. Combust. Flame, **28**, 137 (1977).
7. N. A. BURDETT and A. N. HAYHURST. J. Chem. Soc. Faraday Trans. I, **78**, 2997 (1982).
8. A. N. HAYHURST and N. R. TELFORD. Proc. R. Soc. London A, **322**, 483 (1971).
9. F. WESTLEY. Table of recommended rate constants for chemical reactions occurring in combustion. NSRDS-NBS 67, U.S. Government Printing Office, Washington, DC. 1980.
10. D. L. BAULCH, D. D. DRYSDALE, J. DUXBURY, and S. J. GRANT. Evaluated kinetic data for high temperature reactions. Vol. 3: Homogeneous gas phase reactions of the $O_2$–$O_3$ system, the CO–$O_2$–$H_2$ system, and of sulphur containing species. Butterworths, London. 1976.
11. S. W. BENSON, D. M. GOLDEN, R. W. LAWRENCE, R. SHAW, and R. W. WOOLFOLK. Estimating the kinetics of combustion including reactions involving oxides of nitrogen and sulphur. U.S. Environmental Protection Agency Report No. EPA-600/2-2-75-019. August, 1975.
12. J. A. KERR and M. J. PARSONAGE. Evaluated kinetic data on gas phase hydrogen transfer reactions of methyl radicals. Butterworths, London. 1976.
13. R. P. TURCO, P. HAMILL, O. B. TOON, R. C. WHITTEN, and C. S. KIANG. J. Atmospher. Sci. **86**, 699 (1979).
14. C. K. MOORTGAT and C. E. JUNGE. Pure Appl. Geophys. **115**, 759 (1977).
15. S. D. TANNER. Ph.D. Thesis, York University, Downsview, Ont., Canada M3J 1P3. 1980.
16. D. L. ALBRITTON. Ion–neutral reaction rate constants measured in flow reactions through 1977. Atomic Data and Nuclear Data Tables, **22**, No. 1. July, 1978.
17. D. W. FAHEY, H. BOHRINGER, F. C. FEHSENFELD, and E. E. FERGUSON. J. Chem. Phys. **76**, 1799 (1982).
18. V. K. LAKDAWALA and J. L. MORUZZI. J. Phys. D: Appl. Phys. **14**, 2015 (1981).
19. F. C. FEHSENFELD and E. E. FERGUSON. J. Chem. Phys. **61**, 3181 (1974).
20. D. L. ALBRITTON, I. DOTAN, G. E. STREIT, F. C. FEHSENFELD, and E. E. FERGUSON. Planet. Space Sci. To be published.
21. A. A. VIGGIANO, R. A. PERRY, D. L. ALBRITTON, E. E. FERGUSON, and F. C. FEHSENFELD. J. Geophys. Res. **85**, 4551 (1980).
22. F. C. FEHSENFELD. J. Chem. Phys. **63**, 1686 (1975).
23. E. E. FERGUSON. Acc. Chem. Res. **3**, 402 (1970).
24. F. C. FEHSENFELD and E. E. FERGUSON. J. Chem. Phys. **51**, 3512 (1969).
25. F. C. FEHSENFELD, C. J. HOWARD, and E. E. FERGUSON. J. Chem. Phys. **58**, 5841 (1973).
26. W. LINDINGER, D. L. ALBRITTON, F. C. FEHSENFELD, and E. E. FERGUSON. J. Chem. Phys. **63**, 3238 (1975).
27. H. F. CALCOTE. Eighth Symposium (International) on Combustion. Williams & Wilkins, Baltimore, MD. 1962. p. 184.
28. K. N. BASCOMB, J. A. GREEN, and T. M. SUGDEN. Adv. Mass Spectrom. **2**, 66 (1962).
29. K. A. G. MACNEIL and J. C. J. THYNNE. J. Phys. Chem. **73**, 2960 (1969).
30. J. G. DILLARD and J. L. FRANKLIN. J. Chem. Phys. **48**, 2353 (1968).
31. L. M. BRANSCOMB. Phys. Rev. **148**, 11 (1966).
32. D. FELDMAN. Z. Naturforsch. A**25**, 621 (1970).
33. R. J. CELOTTA, R. A. BENNETT, and J. L. HALL. J. Chem. Phys. **60**, 1740 (1974).
34. H. HOTOP and W. C. LINEBERGER. J. Phys. Chem. Ref. Data, **4**, 539 (1975).
35. S. W. BENSON. Chem. Rev. **78**, 23 (1978).
36. J. W. HASTIE. Combust. Flame, **21**, 187 (1973).